LETTER

doi:10.1038/nature13578

Promoter sequences direct cytoplasmic localization and translation of mRNAs during starvation in yeast

Brian M. Zid[1,2] & Erin K. O'Shea[1,2,3,4]

A universal feature of the response to stress and nutrient limitation is transcriptional upregulation of genes that encode proteins important for survival. Under many such conditions, the overall protein synthesis level is reduced, thereby dampening the stress response at the level of protein expression[1]. For example, during glucose starvation in *Saccharomyces cerevisiae* (yeast), translation is rapidly repressed, yet the transcription of many stress- and glucose-repressed genes is increased[2,3]. Here we show, using ribosomal profiling and microscopy, that this transcriptionally upregulated gene set consists of two classes: one class produces messenger RNAs that are translated during glucose starvation and are diffusely localized in the cytoplasm, including many heat-shock protein mRNAs; and the other class produces mRNAs that are not efficiently translated during glucose starvation and are concentrated in foci that co-localize with P bodies and stress granules, a class that is enriched for mRNAs involved in glucose metabolism. Surprisingly, the information specifying the differential localization and protein production of these two classes of mRNA is encoded in the promoter sequence: promoter responsiveness to heat-shock factor 1 (Hsf1) specifies diffuse cytoplasmic localization and higher protein production on glucose starvation. Thus, promoter sequences can influence not only the levels of mRNAs but also the subcellular localization of mRNAs and the efficiency with which they are translated, enabling cells to tailor protein production to the environmental conditions.

To investigate how cells alter gene expression during stress conditions that elicit an overall reduction in translation, we performed ribosomal profiling[4] on budding yeast cells grown in glucose-replete conditions and glucose-starvation conditions. In agreement with previous results[2], during glucose starvation there was a collapse of polysomes into the 80S monosome peak, indicative of a reduction in global translation (Extended Data Fig. 1a). As reported previously[3], we also observed an inverse correlation between the change in ribosome occupancy upon glucose starvation and the change in mRNA levels (Fig. 1a and Extended Data Fig. 2). For mRNAs whose levels increase during glucose starvation, we observed two classes of behaviour: some upregulated mRNAs ($\log_2$[expression fold change] >2.5) showed a decrease in ribosome occupancy upon glucose starvation ($\log_2$[occupancy fold change] <-1; Fig. 1a, blue dots), whereas others showed an increase in ribosome occupancy that was greater than the median increase for all mRNAs ($\log_2$[ribosome occupancy fold change] >0.09; Fig. 1a, red versus black dots). Moreover, during glucose starvation we observed significantly higher ribosome occupancy in the coding region of the upregulated mRNAs with increased ribosome occupancy than that of the upregulated mRNAs with decreased ribosome occupancy (Fig. 1b; red versus blue genes). The upregulated mRNAs with higher ribosome occupancy were enriched in stress-response mRNAs (16 of 26 genes; $P = 2.4 \times 10^{-9}$), including those encoding heat-shock proteins (Hsp) (Fig. 1a, b and Extended Data Table 1). By contrast, the upregulated mRNAs with lower ribosomal occupancy were enriched for those encoding proteins involved in glucose metabolism (7 of 18 genes; $P = 7.8 \times 10^{-4}$).

Because there is a large reduction in global translation during glucose limitation, our measurements of ribosome occupancy under these conditions are almost certainly overestimates (see Methods). Although this overestimation increases the fold change in ribosome occupancy for all mRNAs, the relative differences between mRNAs are preserved (for example, red versus blue mRNAs). Moreover, we observed these relative differences in ribosome occupancy in different yeast strains and using different RNA isolation methods (Extended Data Fig. 2 and Supplementary Table 1). Thus, mRNAs that are upregulated during glucose starvation have differences in ribosome occupancy.

To determine whether the differences in ribosome occupancy translate into differences in protein production during glucose starvation, we measured protein levels by western blotting. We observed significant increases in proteins derived from the upregulated, higher ribosome occupancy mRNAs *HSP30* and *HSP26* (eightfold and twofold, respectively; Fig. 1c, red bars), but no significant change in protein levels was observed for proteins derived from the lower ribosome occupancy mRNAs *GLC1* and *GSY1* (Fig. 1c, blue bars), even though the mRNAs were induced to similar levels (Fig. 1c). For all upregulated genes that were assessed, we observed a corresponding increase in RNA polymerase II occupancy in their open reading frames (ORFs), suggesting that increased transcription contributes to the upregulation of the corresponding mRNAs during glucose starvation (Extended Data Fig. 3). Thus, upon glucose starvation, transcriptionally upregulated mRNAs have differences in ribosome occupancy, which lead to differences in protein production.

Since some mRNAs localize to messenger ribonucleoprotein (mRNP) foci (including P bodies and stress granules) during glucose limitation[5], one possibility is that mRNA localization influences the ribosome occupancy and translational properties of an mRNA. To investigate whether mRNAs with differences in ribosome occupancy have differences in localization during glucose limitation, we generated fusions of gene coding regions with the MS2 sequence, and we visualized mRNAs using the MS2 coat protein (MS2-CP) fused to green fluorescent protein (GFP), and P bodies using red fluorescent protein (RFP) fused to the P body protein component Dcp2 (ref. 6). In agreement with previous observations[7], *PGK1* and *PDC1* mRNAs, which are abundant pre-starvation, localized predominantly to P bodies after glucose starvation (Fig. 2a, b). By contrast, the transcriptionally upregulated, higher ribosome occupancy mRNAs *HSP26* and *HSP30* remained diffusely localized during glucose starvation, and the transcriptionally upregulated, lower ribosome occupancy mRNAs *GLC3* and *HXK1* became localized to P bodies as well as to other foci (Fig. 2a, b). The formation of foci was dependent on glucose starvation (Extended Data Fig. 4). Stress granules, which contain high concentrations of translation initiation factors, are formed during conditions in which translation is impaired and have been shown to partially overlap with P body foci[8]. Using a Pab1–cyan fluorescent protein (CFP) fusion to visualize stress granules[9], we found that stress granules co-localize with a subset of P bodies, as well as with *GLC3* mRNA foci that were independent of P bodies (Fig. 2c). Therefore, mRNA classes with different

[1]Department of Molecular and Cellular Biology, Harvard University, Cambridge, Massachusetts 02138, USA. [2]Faculty of Arts and Sciences Center for Systems Biology, Harvard University, Cambridge, Massachusetts 02138, USA. [3]Department of Chemistry and Chemical Biology, Harvard University, Cambridge, Massachusetts 02138, USA. [4]Howard Hughes Medical Institute, Harvard University, Cambridge, Massachusetts 02138, USA.

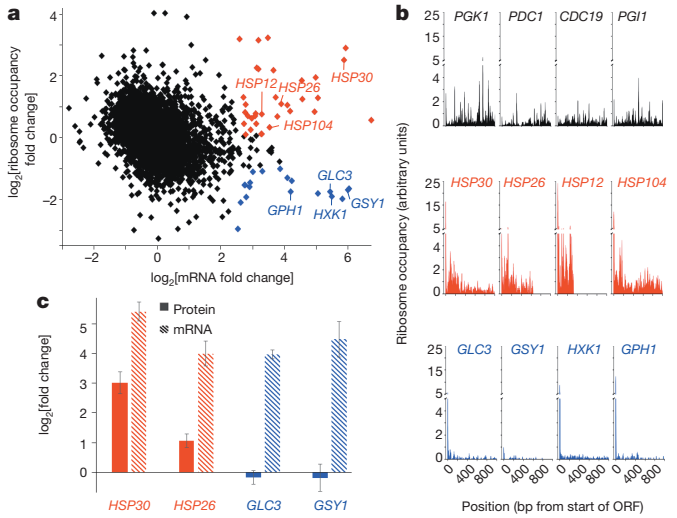

Figure 1 | Ribosomal profiling reveals differences in ribosome occupancy of transcriptionally upregulated mRNAs upon glucose starvation. **a**, Fold change in ribosome occupancy versus fold change in mRNA levels 15 min after cells are transferred to medium lacking glucose compared with levels in glucose-rich medium. mRNAs are represented by individual symbols on the plot. Ribosome occupancy was calculated for the coding region of each mRNA by dividing the total number of ribosome sequence counts in an ORF (normalized to the total number of aligned reads in reads per million reads (RPM)) by the number of mRNA sequence counts (RPM) in the same sequence. RNA sequencing was performed on RNA depleted of ribosomal RNA but not of poly(A)$^+$-selected RNA. Red symbols denote genes that have upregulated mRNA levels ($\log_2$[fold change] >2.5) and a higher ribosome occupancy ($\log_2$[fold change] >0.09). Blue symbols denote genes that have upregulated mRNA levels ($\log_2$[fold change] >2.5) and a lower ribosome occupancy ($\log_2$[fold change] <-1.0). Black symbols represent all other genes in the genome for which measurements were obtained. **b**, Ribosome occupancy (calculated as ribosome reads at each position relative to the average mRNA reads per base pair) for three classes of mRNA: those from genes that had high levels of the corresponding mRNA before glucose limitation (black); those whose mRNA levels increased during glucose limitation and had a higher ribosome occupancy during glucose limitation (red); and those whose mRNA levels increased during glucose limitation and had a lower ribosome occupancy (blue). The time point shown is 15 min after glucose starvation began. **c**, Strains expressing tandem affinity purification (TAP)-tagged versions of the indicated genes[19] grown in glucose-rich medium and then starved of glucose. The mRNA levels were measured by quantitative PCR after 15 min of glucose starvation. The protein abundance, as determined by western blotting, was measured after 30 min of glucose starvation. The mean fold changes in protein abundance (solid bars) and mRNA levels (striped bars) ± s.e.m. were calculated relative to the respective values in glucose-rich medium. The western blotting experiments were performed on four independent biological replicates, and protein levels were normalized to Tub1 protein levels. The Hsp30 and Hsp26 protein levels were significantly higher upon glucose starvation than in glucose-rich medium ($P < 0.05$). A one-tailed, paired *t*-test was used to determine *P* values. The mRNA measurements were made on three independent biological replicates and normalized to *ACT1* mRNA levels. bp, base pairs.

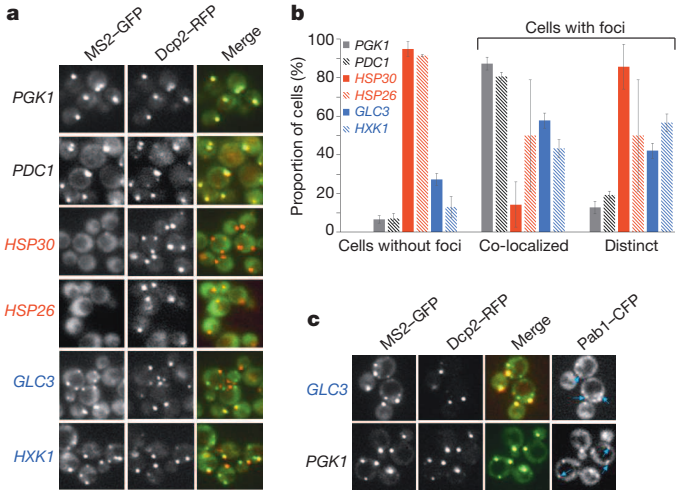

Figure 2 | Glucose starvation induces differences in the localization of mRNAs. **a**, The promoter, 5′ UTR and ORF of genes of interest were fused upstream of the MS2 sequence and the native 3′ UTR, and then mRNA was visualized with fluorescence microscopy using an MS2-coat-protein–GFP fusion reporter after 15 min of glucose starvation. Dcp2–RFP was used to visualize P bodies[6]. **b**, Quantification of mRNA localization to P bodies, as measured by overlap of the MS2 signal with that of the P body marker Dcp2–RFP. Cells without foci were cells that had P body foci but no GFP foci. For cells that contained both GFP (MS2) and RFP (P body) foci, the foci were categorized as either co-localized with P bodies or not overlapping with (distinct from) P bodies. The values are presented as mean ± s.e.m. of the data from Fig. 2a, measured on a minimum of 25 cells in quadruplicate (two biological replicates with two technical replicates per sample). Cells expressing *HSP30* or *HSP26* mRNA had fewer foci than cells expressing *PGK1*, *PDC1*, *GLC3* or *HXK1* mRNAs ($P < 0.01$). Cells expressing *GLC3* or *HXK1* mRNA had significantly more distinct foci than those expressing *PGK1* or *PDC1* mRNA ($P < 0.05$ for all comparisons). Since few cells expressing *HSP30* or *HSP26* mRNA had foci, these cells were excluded from statistical analyses because of the high measurement variability. A two-tailed, two-sample unequal variance *t*-test was performed to determine the *P* values. **c**, Pab1–CFP was used to visualize stress granule localization[10] after 30 min of glucose starvation. The blue arrows point to stress granules (Pab1–CFP signals) that do not co-localize with P bodies (Dcp2–RFP signal). In the *GLC3-MS2* strain, the Pab1–CFP stress granule foci overlapped with the GFP foci that were distinct from P bodies.

ribosome occupancy and protein production properties have distinct subcellular localization patterns.

To investigate whether the timing of mRNA production relative to glucose limitation contributes to mRNA localization, we analysed the localization and translation of a reporter gene that consisted of the doxycycline-inducible Tet-On promoter controlling the expression of *lacZ-MS2*. When *lacZ-MS2* was induced before glucose starvation and cells were then starved, the mRNAs co-localized predominantly with P bodies (Extended Data Fig. 5a, b): this is consistent with the published observation that mRNAs that exist pre-starvation become localized to P bodies upon glucose limitation[7]. By contrast, when the mRNA was induced only during glucose starvation, it formed foci that co-localized with P bodies and foci distinct from P bodies, a pattern similar to that of transcriptionally upregulated, lower ribosome occupancy mRNAs (Fig. 2, blue mRNAs). These results were not sensitive to the timing of induction during starvation or to the level of induction (over a range from 4-fold to 30-fold induction) (Extended Data Fig. 5). Thus, the timing of mRNA production relative to glucose limitation influences cytoplasmic mRNA localization.

The timing of mRNA production can influence whether mRNAs are localized exclusively to P bodies, but it is unclear what causes the differential localization and translation of transcriptionally upregulated, higher and lower ribosome occupancy mRNAs. To determine whether we could identify signals present in the mRNA itself, we fused the promoter and/or 5′ untranslated region (UTR) of each gene to a constant ORF, *CFP*, and found that these fusions exhibited the same patterns of localization as the native ORFs, suggesting that the information specifying localization was contained in these elements (Fig. 3a, b and Extended Data Fig. 6a). To determine whether the promoter or 5′ UTR was sufficient to determine localization, we generated chimaeras between the *HSP26* promoter and the *GLC3* 5′ UTR, as well as between the *GLC3* or *HXK1* promoter and the *HSP26* 5′ UTR. In each case the promoter was sufficient to recapitulate the localization observed for the native gene (Fig. 3a, b and Extended Data Fig. 6a). Changes in the transcription start sites are not likely to account for these observations, as we did not observe significant differences in the 5′ ends of the mRNAs produced from the chimaeras

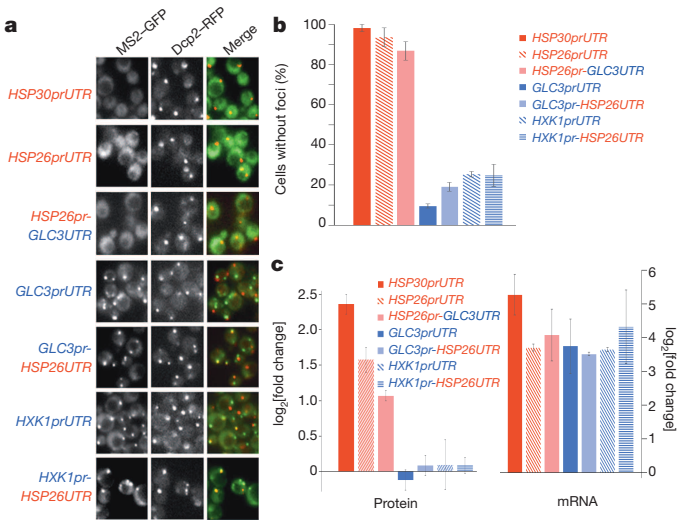

Figure 3 | Differential localization of mRNAs is determined by the promoter. **a**, The promoter (pr) and 5′ UTR of the indicated genes were fused upstream of *CFP–MS2*, and localization of the resultant mRNA was visualized 15 min after glucose starvation. **b**, Quantification of the data shown in Fig. 3a. The values are presented as the mean ± s.e.m. measured on a minimum of 30 cells in quadruplicate (two biological replicates with two technical replicates per sample). There were significantly fewer foci in the cells containing *HSP30*- or *HSP26*-promoted mRNAs (red bars) than in cells with *GLC3*- or *HXK1*-promoted mRNAs (blue bars) ($P < 0.01$). A two-tailed, two-sample unequal variance *t*-test was performed to determine the *P* values. **c**, Protein expression directed by the indicated promoter–UTR combinations was measured by western blotting using an anti-GFP antibody that recognizes CFP. The protein levels were measured after 30 min of glucose starvation and in glucose-rich medium, and the fold change in protein abundance was calculated. *MS2-CP–GFP*(3×) driven by the *MYO2* promoter was used as a loading control for western blotting. The protein fold changes are presented as mean ± s.e.m. and were calculated from four independent biological replicates. The levels of the proteins produced from *HSP30*- and *HSP26*-promoted mRNAs (red bars) significantly increased upon glucose starvation compared with in glucose-rich medium ($P < 0.01$). A one-tailed, paired *t*-test was used to determine the *P* values. The fold change in mRNA levels was determined after 15 min of glucose starvation versus growth in glucose-rich medium, measured by qPCR using *CFP* primers and *ACT1* levels to normalize expression. The mRNA fold-change values are presented as mean ± s.e.m. and were calculated from three independent biological replicates.

(Extended Data Table 2). To determine whether the correlation between localization and translation that we observed previously for native mRNAs (Figs 1 and 2) also holds for these chimaeras, we measured protein production and found that the *HSP* promoters that specify diffuse mRNA localization result in a larger increase in protein production during glucose starvation (Fig. 3c, red bars). By contrast, although the focus-forming *GLC3* and *HXK1* promoters drive levels of mRNA induction similar to those driven by the *HSP26* promoter, during glucose starvation there was no significant increase in protein production from mRNAs driven by these promoters (Fig. 3c, blue bars). Thus, promoters can influence gene expression through means other than by simply controlling mRNA induction.

To identify specific promoter sequences that influence mRNA localization and protein production, we made promoter chimaeras from *GLC3* and *HSP26* and used these chimaeras to drive the expression of *CFP–MS2*. Two sets of transcription factors that activate transcription upon glucose starvation are Msn2 and Msn4, which bind to stress-response elements (STREs)[10], and Hsf1, which binds to heat-shock elements (HSEs)[11]. We generated chimaeric promoters containing combinations of STREs and HSEs from the *GLC3* and *HSP26* promoters and analysed mRNA localization of mRNAs translated from reporter constructs. We found that mRNA reporters whose expression was controlled by chimaera 1 or 4 were induced in response to glucose limitation, with the mRNA forming foci in a high percentage of cells, but they produced no significant change in CFP protein levels (Fig. 4b–d and Extended Data Fig. 6b): these chimaeras exclude many of the HSE sites contained in the *HSP26* promoter but include at least three STRE sites. By contrast, mRNA reporters whose expression was controlled by chimaera 2 or 3 were also induced in response to glucose limitation, but the mRNA had generally diffuse localization (Fig. 4b–d and Extended Data Fig. 6b), more similar to that of the full-length *HSP26* promoter; they also produced significant increases in protein levels upon glucose starvation (Fig. 4d). All four chimaeras resulted in similar levels of mRNA induction, and chimaeras 1 and 2 led to similar absolute mRNA levels after 15 min of glucose starvation (Fig. 4d and Extended Data Fig. 7a). The sequence in common to chimaeras 2 and 3 is a 90-base-pair region that contains several HSEs[12].

To determine whether Hsf1 responsiveness correlates with the diffuse localization of the chimaeras, we treated cells expressing different reporters with azetidine-2-carboxylate (AZC), a proline analogue that robustly increases *HSF1* transcriptional activity with low activation of the STRE response[13]. The full-length *HSP26* and *GLC3* promoters both exhibited strong induction in response to glucose starvation, but only the *HSP26* promoter showed robust induction in response to AZC treatment (Extended Data Fig. 7b). All four of the chimaeric promoters responded similarly to glucose starvation, but only chimaeras 2 and 3 showed greater than 20-fold induction upon treatment with AZC (Extended Data Fig. 7b). Thus, responsiveness to Hsf1 correlates with, and may contribute to, diffuse mRNA localization and protein production during glucose starvation.

Our ability to assess whether Hsf1 is necessary for diffuse localization was precluded by the *S. cerevisiae HSF1* deletion strain being non-viable[14]; however, we can infer the role of Hsf1 by examining the localization of mRNAs and the protein production resulting from constructs that contain different combinations of STREs and HSEs (Fig. 4b, schematic, and Extended Data Fig. 8). *CFP–MS2* expressed under the control of a synthetic promoter that contains only STREs formed many foci during glucose limitation (Fig. 4b, bottom panel, Fig. 4c, right, and Extended Data Fig. 6b). The addition of three HSEs to this synthetic STRE promoter was sufficient to switch the mRNA localization from foci to diffuse localization (Fig. 4b, bottom panel, Fig. 4c, right, and Extended Data Fig. 6b). The synthetic reporter containing HSE binding sites resulted in more protein production during glucose starvation than a synthetic promoter containing only STREs, even though the two promoters had similar levels of mRNA induction (Fig. 4d). We conclude that HSE binding sites, probably functioning through the transcription factor Hsf1, influence mRNA localization and translation upon glucose starvation.

Our data suggest that promoter sequences and the action of select transcription factors in the nucleus can influence mRNA localization and translation upon glucose starvation (Fig. 4e). A link between transcriptional regulation and cytoplasmic localization may be a general adaptation during times of stress, enabling cells to coordinately regulate the production of entire classes of proteins. Under non-stress conditions, the upregulation of a class of transcripts by a transcription factor would produce similar amounts of protein from each of the mRNAs, as translation would proceed at a generally high rate. Under stressful conditions, when translation is reduced overall, selective translation may be required to produce proteins that are needed for adaptation to the new conditions. In the case of glucose starvation, Hsf1 targets that encode cytoprotective proteins, such as chaperones, may need to be produced as soon as possible to help the cells cope with the stress, but alternative glucose metabolism genes may be superfluous when no carbon source is present. The induction of mRNA without a concomitant increase in the protein level of genes involved in glucose metabolism may allow cells to more rapidly produce proteins upon reintroduction of a carbon source. Intriguingly, the localization of *HSP70* and *HSP90* mRNA in stressed yeast and mammalian cells appears to be similar: these mRNAs are largely excluded from stress granules during cellular stress in mammalian cells[15,16]. Previous studies have shown that the promoter can influence the stability of an mRNA through co-transcriptional loading of an

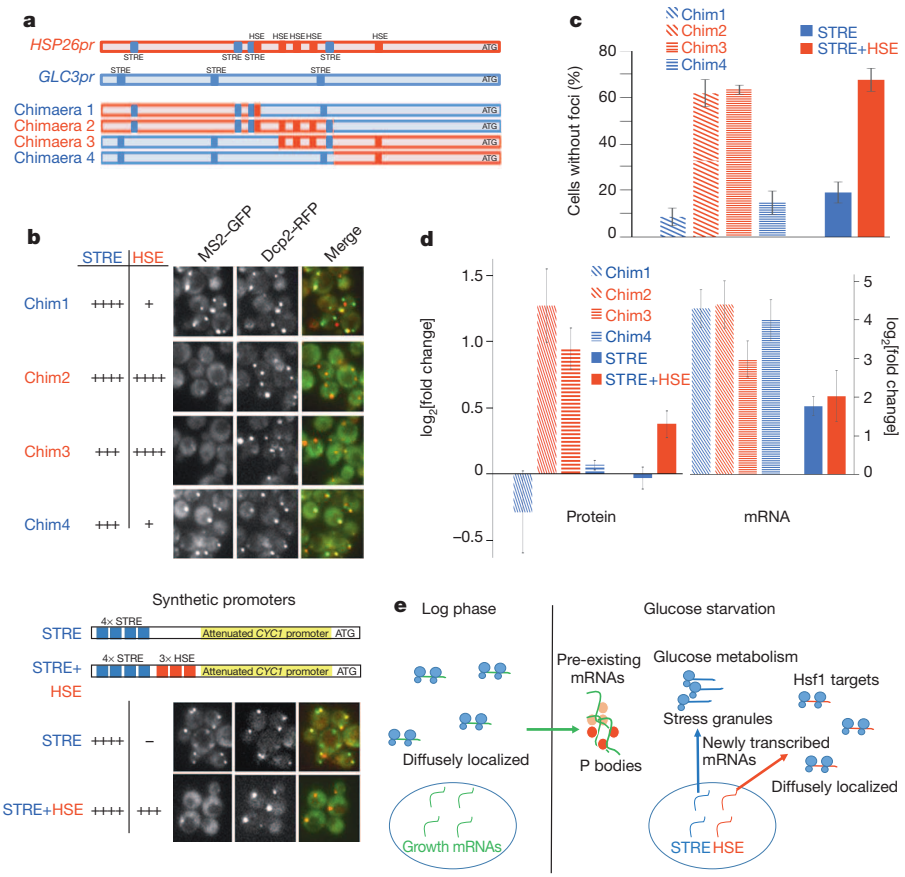

Figure 4 | Promoter elements influence mRNA translation efficiency and localization. **a**, Schematic of the promoter regions that control the expression of *CFP–MS2*. The HSE sites are taken from ref. 12. **b**, Localization of *CFP–MS2* mRNA driven by chimaeric (Chim) *HSP26* and *GLC3* promoters or synthetic promoters (STRE or STRE+HSE) visualized after 15 min of glucose starvation. Dcp2–RFP was used to visualize P bodies[6]. **c**, Quantification of the data shown in Fig. 4b. The values are presented as the mean ± s.e.m. and were measured on a minimum of 25 cells in quadruplicate (two biological replicates with two technical replicates per sample). Chim1- or Chim4-promoted mRNAs showed more focus formation than did Chim2- or Chim3-promoted mRNAs ($P < 0.05$). The promoter containing only STRE (and no HSE) resulted in mRNA showing more focus formation than did the STRE+HSE-promoted mRNA ($P < 0.01$). A two-tailed, two-sample unequal variance *t*-test was performed to determine the *P* values. **d**, Protein expression directed by the different promoters was measured by western blotting using an anti-GFP antibody that recognizes CFP. The protein levels were measured after 30 min of glucose starvation, and the fold change was calculated relative to measurements in glucose-rich medium. *MS2-CP–GFP*(3×) driven by the *MYO2* promoter was used as a loading control for western blotting. The protein fold-change values are presented as the mean ± s.e.m. and were calculated from five independent biological replicates for the chimaeric promoters and seven independent biological replicates for the synthetic promoters. The levels of proteins produced from Chim2-, Chim3- and STRE+HSE-driven mRNAs (red bars) were significantly increased upon glucose starvation compared with in glucose-rich medium ($P < 0.05$). A one-tailed, paired *t*-test was used to determine the *P* values. The fold change in mRNA levels was measured after 15 min of glucose starvation versus growth in glucose-rich medium, by using qPCR with *CFP* primers and with expression normalized to *ACT1* levels. The mRNA fold-change values are presented as the mean ± s.e.m. and were calculated from three independent biological replicates. **e**, mRNAs that are actively transcribed during the logarithmic (log) phase, such as *PDC1* and *PGK1*, localize to P bodies during glucose starvation. mRNAs whose expression is activated by Hsf1 through HSE elements, including *HSP30* and *HSP26*, are diffusely localized during glucose starvation and result in high levels of protein production. mRNAs such as *GLC3* and *HXK1*, which are upregulated by STREs independently of Hsf1, localize to P bodies and stress granules and are poorly translated during glucose starvation.

accessory protein onto the mRNA[17,18]. A similar phenomenon may be operating here, whereby transcription factors load RNA-binding proteins that direct mRNA localization, or there may be *cis* alterations to the mRNA, such as to its poly(A)$^+$ tail length or methylation, that influence its fate. Future studies will reveal aspects of these mechanisms, as well as whether this phenomenon is conserved in other eukaryotes.

Online Content Methods, along with any additional Extended Data display items and Source Data, are available in the online version of the paper; references unique to these sections appear only in the online paper.

Received 30 October 2013; accepted 11 June 2014.
Published online 3 August 2014.

1. Simpson, C. E. & Ashe, M. P. Adaptation to stress in yeast: to translate or not? *Biochem. Soc. Trans.* **40,** 794–799 (2012).
2. Ashe, M. P., De Long, S. K. & Sachs, A. B. Glucose depletion rapidly inhibits translation initiation in yeast. *Mol. Biol. Cell* **11,** 833–848 (2000).
3. Arribere, J. A., Doudna, J. A. & Gilbert, W. V. Reconsidering movement of eukaryotic mRNAs between polysomes and P bodies. *Mol. Cell* **44,** 745–758 (2011).
4. Ingolia, N. T., Ghaemmaghami, S., Newman, J. R. S. & Weissman, J. S. Genome-wide analysis *in vivo* of translation with nucleotide resolution using ribosome profiling. *Science* **324,** 218–223 (2009).
5. Decker, C. J. & Parker, R. P-bodies and stress granules: possible roles in the control of translation and mRNA degradation. *Cold Spring Harb. Perspect. Biol.* **4,** a012286 (2012).
6. Brengues, M., Teixeira, D. & Parker, R. Movement of eukaryotic mRNAs between polysomes and cytoplasmic processing bodies. *Science* **310,** 486–489 (2005).
7. Teixeira, D., Sheth, U., Valencia-Sanchez, M. A., Brengues, M. & Parker, R. Processing bodies require RNA for assembly and contain nontranslating mRNAs. *RNA* **11,** 371–382 (2005).
8. Buchan, J. R. & Parker, R. Eukaryotic stress granules: the ins and outs of translation. *Mol. Cell* **36,** 932–941 (2009).
9. Hoyle, N. P., Castelli, L. M., Campbell, S. G., Holmes, L. E. & Ashe, M. P. Stress-dependent relocalization of translationally primed mRNPs to cytoplasmic granules that are kinetically and spatially distinct from P-bodies. *J. Cell Biol.* **179,** 65–74 (2007).

10. Martínez-Pastor, M. T. *et al.* The *Saccharomyces cerevisiae* zinc finger proteins Msn2p and Msn4p are required for transcriptional induction through the stress response element (STRE). *EMBO J.* **15,** 2227–2235 (1996).
11. Hahn, J.-S. & Thiele, D. J. Activation of the *Saccharomyces cerevisiae* heat shock transcription factor under glucose starvation conditions by Snf1 protein kinase. *J. Biol. Chem.* **279,** 5169–5176 (2004).
12. Susek, R. E. & Lindquist, S. Transcriptional derepression of the *Saccharomyces cerevisiae HSP26* gene during heat shock. *Mol. Cell. Biol.* **10,** 6362–6373 (1990).
13. Trotter, E. W. *et al.* Misfolded proteins are competent to mediate a subset of the responses to heat shock in *Saccharomyces cerevisiae*. *J. Biol. Chem.* **277,** 44817–44825 (2002).
14. Wiederrecht, G., Seto, D. & Parker, C. S. Isolation of the gene encoding the *S. cerevisiae* heat shock transcription factor. *Cell* **54,** 841–853 (1988).
15. Kedersha, N. & Anderson, P. Stress granules: sites of mRNA triage that regulate mRNA stability. *Biochem Soc. Trans.* **30,** 963–969 (2002).
16. Stöhr, N. *et al.* ZBP1 regulates mRNA stability during cellular stress. *J. Cell Biol.* **175,** 527–534 (2006).
17. Bregman, A. *et al.* Promoter elements regulate cytoplasmic mRNA decay. *Cell* **147,** 1473–1483 (2011).
18. Trcek, T., Larson, D. R., Moldón, A., Query, C. C. & Singer, R. H. Single-molecule mRNA decay measurements reveal promoter-regulated mRNA stability in yeast. *Cell* **147,** 1484–1497 (2011).
19. Ghaemmaghami, S. *et al.* Global analysis of protein expression in yeast. *Nature* **425,** 737–741 (2003).

Supplementary Information is available in the online version of the paper.

Acknowledgements We thank A. Subramaniam, S. Mukherji, V. Denic, B. Stern and M. Waldram for feedback on the paper, members of the O'Shea, Denic, and Calarco laboratories for discussions, and C. Daly for sequencing assistance. This research was supported by the American Cancer Society and the New England Division Funding A Cure initiative (B.M.Z.) and the Howard Hughes Medical Institute (E.K.O.).

Author Contributions B.M.Z. collected and analysed the data. B.M.Z. and E.K.O. designed the experiments and wrote the manuscript.

Author Information All raw sequencing data have been deposited in the Gene Expression Omnibus database under accession number GSE56622. Reprints and permissions information is available at www.nature.com/reprints. The authors declare no competing financial interests. Readers are welcome to comment on the online version of the paper. Correspondence and requests for materials should be addressed to E.K.O. (Erin_Oshea@harvard.edu).

METHODS

Yeast strains and growth. All yeast strains are listed in Supplementary Table 2. For the ribosomal profiling experiments presented in Fig. 1, the yeast strain BY4741 (Euroscarf) (MAT**a** *his3Δ1 leu2Δ0 met15Δ0 ura3Δ0*) was grown at 30 °C in batch culture with shaking at 125 r.p.m. in synthetic complete glucose medium (SCD medium) and synthetic complete medium lacking glucose (SC medium). Yeast cells were randomly chosen by taking half of the cells from a culture for glucose starvation and the other half for assessment under glucose-replete conditions. There was no blinding to the group that the yeast were allocated to. Ribosomal profiling and RNA sequencing (RNA-seq) were repeated under the same growth conditions using the yeast strain EY0690 (W303 MAT**a** *trp1-1 leu2-3 ura3-1 his3-11 can1-100*), and similar results were obtained (Extended Data Fig. 2 and Supplementary Table 1).

The yeast strain background W303 (EY0690) was used for all microscopy experiments. To image mRNAs, the 12× MS2 sequence was excised from the MS2L construct[20] and placed in the *LEU2*-marked integration vector pRS305. The *ADH1* 3′ UTR was cloned downstream of this sequence, and gene-specific sequences were cloned upstream of the MS2 sequence by Gibson Assembly[21]. Integration was performed by cleaving the resultant plasmids within the *LEU2* gene with EcoRV and transforming the linear fragment into a yeast strain (EY2888) containing *MS2-CP–GFP*(3×)[20] under the control of the *MYO2* promoter integrated at the *HIS3* locus. Dcp2 was tagged with RFP, and Pab1 with the CFP mTurquoise2 by carboxy-terminal chromosomal integration of PCR products, including auxotrophic or antibiotic markers flanked by 40 base pairs (bp) of sequence found directly upstream and downstream of the gene, followed by selection on the appropriate medium[22]. *TETO7-lacZ-MS2-ADH1_3′ UTR* was integrated into the EY2888 strain at the *LEU2* locus with the addition of the rtTA activator (Tet-On) under the control of the *ERV14* promoter (EB1674). Doxycycline was added to a final concentration of 20 μg ml^{-1} either 15 min before glucose starvation or at the time of glucose starvation. A yeast-codon-optimized CFP reporter (*SCFP3A*)[23] was used to generate a uniform ORF for localization constructs driven by various promoters (Figs 3 and 4). To determine Hsf1 responsiveness, AZC was added to a final concentration of 10 mM to cells at an optical density at 600 nm (OD_{600}) of ~0.2, and cells were incubated with shaking for 2 h.

Chimaeric *HSP26* and *GLC3* promoters, shown in Fig. 4a, were made by fusion PCR of the indicated promoter regions (Supplementary Table 2) and were inserted upstream of *CFP-MS2-ADH1_3′ UTR*. Synthetic reporters were created by Gibson Assembly of a 4× STRE with or without a 3× HSE element followed by an attenuated *CYC1* promoter[24] upstream of *CFP-MS2-ADH1_3′ UTR* (Extended Data Fig. 8). A Mig1-binding site[25] (AAAAATGCGGGG) was included 5′ of the STREs to reduce leaky expression under glucose-rich conditions.

Ribosomal profiling and RNA-seq. Ribosomal profiling and RNA-seq were performed as described previously[4]. We performed two ribosomal profiling experiments for BY4741 and two for EY0690. Yeast were grown in SCD at 30 °C to an OD_{600} between 0.3 and 0.4. Then, cells were collected by filtration, resuspended in SC medium (lacking glucose) and grown for 15 min. Cycloheximide was added to a final concentration of 100 μg ml^{-1} for 1 min with continued shaking at 30 °C, and cells were then harvested. Cells were pulverized in a PM 100 ball mill (Retsch), and extracts were digested with RNase I followed by the isolation of ribosome-protected fragments either by purifying RNA from the monosome fraction of a sucrose gradient (BY4741 two samples) or by using a sucrose cushion (EY0690 two samples). Isolated 28-base sequences were polyadenylated, and reverse transcription was performed using either OTi225 (BY4741) or OTi9pA (EY0690) (Supplementary Table 3). OTi9pA allowed samples to be multiplexed at subsequent steps. RNA-seq was performed on RNA depleted of rRNA using a yeast Ribo-Zero kit (Epicentre) (EY0690, one experiment), total RNA (BY4741 and EY0690, one experiment each) or poly(A)$^+$-selected RNA using Oligo(dT) Dynabeads (Invitrogen) (BY4741 and EY0690, two independent samples each). rRNA-depleted RNA and total RNA from EY0690 had a high Pearson correlation between samples ($r > 0.9$), so these sequences were combined to give higher sequence coverage for the mRNA sample. BY4741 samples were sequenced on an Genome Analyzer II (Illumina), while EY0690 samples were multiplexed and sequenced on a HiSeq analyser (Illumina) (both at the FAS Center for Systems Biology Core Facility). All raw sequencing data are available at NCBI GEO, with accession number GSE56622.

To analyse the ribosomal profiling and RNA-seq sequences, reads were trimmed of the 3′ run of poly(A)s and then aligned against *S. cerevisiae* rRNA sequences using Bowtie sequence aligner[26]. Reads that did not align to rRNA sequences were aligned against the full *S. cerevisiae* genome. Reads that had an unambiguous alignment with less than three mismatches were used in the measurements of ribosome occupancy and mRNA levels. Since there were many reads mapping to the initiation region (−16 bp to +20 bp in relation to the AUG; Extended Data Fig. 1b), the ribosome occupancy for each mRNA was calculated by taking the total number of ribosome reads (normalized to the total number of aligned reads in reads per million reads (RPM)) in the downstream region (+20 bp from the AUG to the end of the ORF; Extended Data Fig. 1b) and dividing this by the number of mRNA reads (RPM) in the same region. The ribosome occupancy along the mRNA (Fig. 1b) was calculated by dividing the ribosome read counts at each base pair along the gene by the average number of mRNA reads per base pair for each gene. Because there is a large reduction in global translation during glucose limitation, our measurements of ribosome occupancy under these conditions are almost certainly overestimates. This arises because even when there is a large reduction in ribosomes associated with mRNAs, as seen by the collapse in the polysome profile during glucose starvation (Extended Data Fig. 1), we isolated and sequenced the same number of ribosome-protected sequence reads. Although this has the effect of increasing ribosome occupancy values for all genes, the relative differences between mRNAs remain (for example, red (*HSP* mRNAs) versus blue (glucose metabolism mRNAs)).

To reduce sampling error, a cut-off of 30 or more reads in the downstream region was set for RNA-seq during glucose starvation. Since we focused on mRNAs that were upregulated during glucose limitation and since many of these genes are poorly expressed in glucose-rich conditions, we set a cut-off of four or more reads for RNA-seq during glucose-rich conditions, as well as four or more reads for ribosomal profiling in both glucose-rich and glucose-starvation conditions. Even with such a low number of reads as a cut-off, there was a large overlap between ribosomal profiling and non-poly(A)$^+$-selected RNA-seq experiments performed in BY4741 and EY0690 at both the individual gene level and the gene ontology class level for the different categories of upregulated mRNAs (Extended Data Table 1 and Supplementary Table 1). At the individual gene level, 21 of the 33 upregulated, higher ribosome occupancy genes classified from BY4741 were in the same category for the EY0690 data, while only 2 genes switched to the upregulated, lower ribosome occupancy category (Supplementary Table 1). For lower ribosome occupancy mRNAs, 13 of the 19 genes classified as such in BY4741 were also found in the same category for EY0690, while only 2 genes switched to the upregulated, higher ribosome occupancy category (Supplementary Table 1). Extended Data Fig. 2 shows the data from all four ribosomal profiling data sets, together with the six mRNA preparations that include both poly(A)$^+$-selected and non-poly(A)$^+$-selected mRNA.

Polysome analysis. Sucrose density gradients (10–50%) were prepared and measured using a BioComp Gradient Station (BioComp Instruments) according to the manufacturer's instructions. Sucrose solutions were prepared in 20 mM Tris, pH 8.0, 140 mM KCl, 5 mM $MgCl_2$, 0.5 mM dithiothreitol (DTT) and 50 U ml^{-1} SUPERase·In (Ambion). Samples were loaded onto gradients and spun for 3 h at 35,000 r.p.m. at 4 °C in an SW41 rotor (Beckman Coulter). Samples were passed through a BioComp Gradient Station, and the absorbance at 260 nm was read using an Econo UV Monitor (Bio-Rad).

Microscopy. Cells were grown to an OD_{600} between 0.3 and 0.4 in SCD at 30 °C and then washed and resuspended in SC. After 15 min, cells were concentrated and imaged using an Axiovert 200M inverted microscope (Zeiss) with a Cascade 512 cooled charge-coupled (CCD) camera (Photometrics) and an oil-immersion 63× objective. A custom MATLAB script was written to measure co-localization of GFP mRNA foci and RFP P body foci. In brief, a threshold mask was set for individual cells using the Otsu Thresholding Filter[27] and subsequently used to create a binary image. The centroid of each focus was then obtained using the regionprops command. If no mRNA foci were found, the cell was counted as without foci. If there were one or more mRNA foci, the minimum distance between each mRNA focus and every P body foci in the cell was calculated. If this distance was less than or equal to 1.5 pixels, the focus was considered to be co-localized; otherwise, it was considered non-overlapping and distinct. *P* values were calculated using a two-tailed, two-sample unequal variance *t*-test to account for possible differences in variance, which may arise from unrelated data[28]. For stress granule visualization, cells were imaged after 30 min of glucose starvation to observe clear stress granule formation.

Quantitative PCR (qPCR). RNA was extracted using the MasterPure Yeast RNA Purification Kit (Epicentre). cDNA was prepared using SuperScript III Reverse Transcriptase (Invitrogen) with a combination of oligo(dT) primers and random hexamers according to the manufacturer's instructions. mRNA abundance was determined by qPCR using SYBR Green PCR Master Mix (Applied Biosystems) and primers specific for each transcript (Supplementary Table 3). The mRNA levels were normalized to *ACT1* abundance, and the fold change between glucose-starvation and glucose-rich conditions was calculated.

Chromatin immunoprecipitation (ChIP). ChIP–qPCR experiments were conducted as previously described[29] with the following differences. Rpb3–TAP (tandem affinity purification)[19] was used to determine RNA polymerase II occupancy in glucose-rich conditions and after 15 min of glucose starvation. Rpb3–TAP was immunoprecipitated using IgG Sepharose Fast Flow (GE Healthcare). Input and immunoprecipitated samples were assayed by qPCR to assess the extent of RNA polymerase II occupancy in different genomic regions. Primer pairs against the indicated ORFs, as well as an untranscribed telomeric region (Supplementary Table 3), were used to determine PCR efficiencies during glucose-rich and glucose-starvation conditions.

Western blotting. Strains were grown in the appropriate medium and then centrifuged at 4,000*g* for 2 min. Pellets were resuspended in Buffer A (0.5% Triton X-100, 150 mM NaCl, 1 mM EDTA and 50 mM HEPES, pH 7.4) followed by lysis with glass beads at 4 °C and centrifugation at 5,000*g* for 5 min. The crude extract was then resolved by SDS–PAGE, and a rabbit polyclonal antibody specific for calmodulin-binding peptide (A00635-40, GenScript) was used to detect TAP-tagged proteins. A mouse anti-α-tubulin antibody (12G10, Developmental Studies Hybridoma Bank) was used as a loading control. CFP and GFP were detected using a rabbit polyclonal antibody against GFP (A-6455, Invitrogen), with the *pMYO2*-driven *MS2-CP–GFP*(3×) used as a loading control. To determine whether there was an increase in protein levels from glucose-replete conditions to glucose-starvation conditions, a one-tailed, paired *t*-test was used. The Shapiro–Wilk statistic was computed to test for normality in these small sample sizes of four to seven replicates. These sample sizes are commonly used to measure differences in protein levels.

5′ RACE. The transcriptional start site was determined for various promoters using the ExactSTART Eukaryotic mRNA 5′ RACE Kit (Epicentre). An adaptor oligoribonucleotide (5′ adaptor) was ligated to the 5′ end of the RNA, and cDNA was synthesized using an oligo(dT) primer that contained another adaptor sequence (3′ adaptor). The 5′ region of the mRNA was amplified by PCR using a kit-provided 5′ adaptor primer (5′-TCATACACATACGATTTAGGTGACACTATAGAGCG GCCGCCTGCAGGAAA-3′), and a CFP-specific primer (Supplementary Table 3). The PCR products were cloned into the pCR4-TOPO vector (Invitrogen) and were sequenced (Eton).

20. Haim-Vilmovsky, L. & Gerst, J. E. m-TAG: a PCR-based genomic integration method to visualize the localization of specific endogenous mRNAs *in vivo* in yeast. *Nature Protocols* **4,** 1274–1284 (2009).
21. Gibson, D. G. *et al.* Enzymatic assembly of DNA molecules up to several hundred kilobases. *Nature Methods* **6,** 343–345 (2009).
22. Longtine, M. S. *et al.* Additional modules for versatile and economical PCR-based gene deletion and modification in *Saccharomyces cerevisiae*. *Yeast* **14,** 953–961 (1998).
23. Hansen, A. S. & O'Shea, E. K. Promoter decoding of transcription factor dynamics involves a trade-off between noise and control of gene expression. *Mol. Syst. Biol.* **9,** 704 (2013).
24. Brandman, O. *et al.* A ribosome-bound quality control complex triggers degradation of nascent peptides and signals translation stress. *Cell* **151,** 1042–1054 (2012).
25. Lutfiyya, L. L. *et al.* Characterization of three related glucose repressors and genes they regulate in *Saccharomyces cerevisiae*. *Genetics* **150,** 1377–1391 (1998).
26. Langmead, B., Trapnell, C., Pop, M. & Salzberg, S. L. Ultrafast and memory-efficient alignment of short DNA sequences to the human genome. *Genome Biol.* **10,** R25 (2009).
27. Otsu, N. A threshold selection method from gray-level histograms. *IEEE Trans. Syst. Man Cybern.* **9,** 62–66 (1979).
28. Ruxton, G. D. The unequal variance *t*-test is an underused alternative to Student's *t*-test and the Mann–Whitney *U* test. *Behav. Ecol.* **17,** 688–690 (2006).
29. Cook, K. E. & O'Shea, E. K. Hog1 controls global reallocation of RNA Pol II upon osmotic shock in *Saccharomyces cerevisiae*. *G3 (Bethesda)* **2,** 1129–1136 (2012).

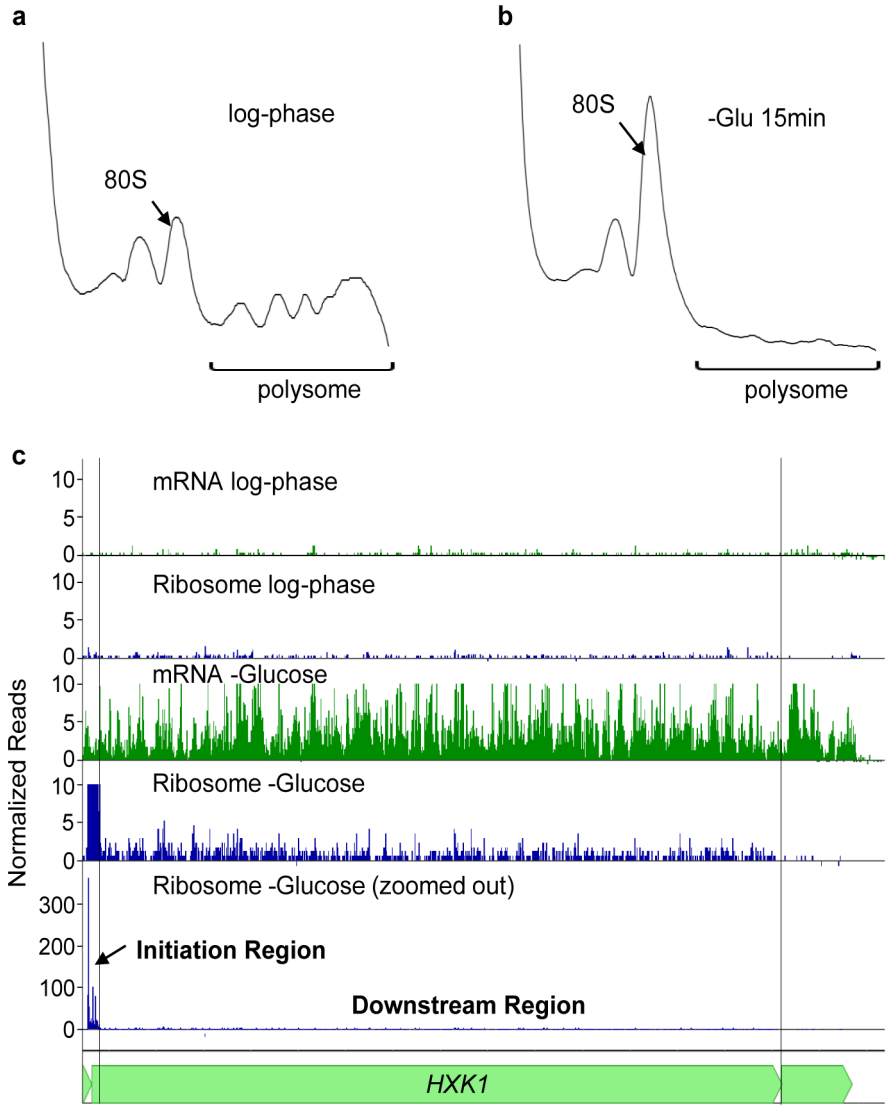

Extended Data Figure 1 | Glucose starvation causes a reduction in overall translation, along with gene-specific changes in ribosome and mRNA read density. **a**, Sedimentation profile of logarithmic-phase cells of strain BY4741 grown in SCD medium. The arrow marks the sedimentation of the 80S ribosome. **b**, Sedimentation profile of cells of strain BY4741 grown in SCD medium and then transferred to the same medium lacking glucose for 15 min. **c**, Ribosome and mRNA read density across the *HXK1* mRNA during logarithmic-phase growth in glucose-rich conditions and after 15 min of glucose starvation. For the tracks labelled "mRNA", the number of mRNA reads is shown normalized to the total number of sequence reads for that sample (in reads per million reads (RPM)). For the tracks labelled "Ribosome", the number of ribosome reads is shown normalized to the total number of reads for that sample (in RPM). The initiation region was defined as a 36-base-pair (bp) region that contains 16 bp upstream of the AUG and 20 bp downstream. The downstream region is defined as the rest of the ORF.

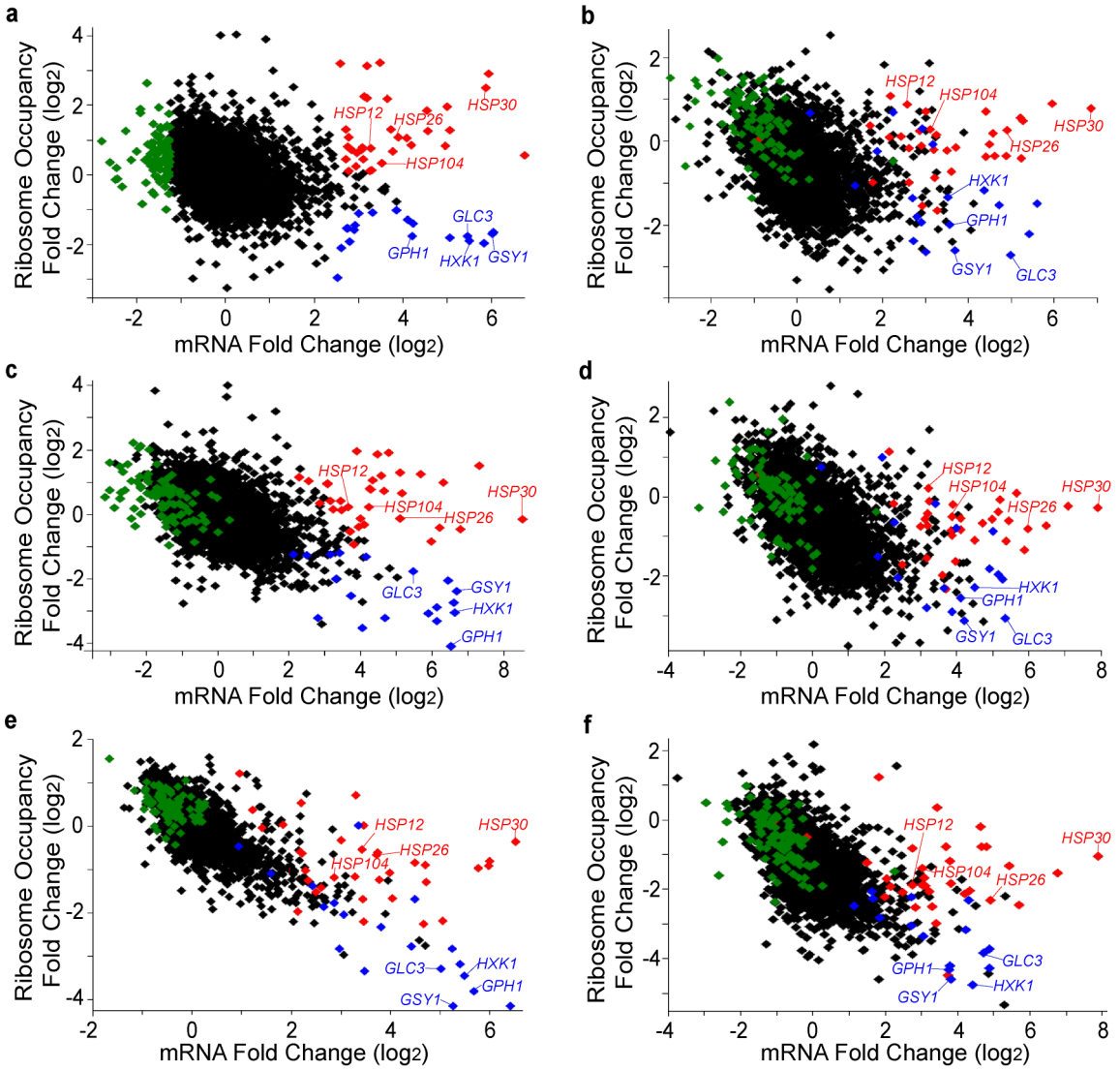

Extended Data Figure 2 | Differences in ribosome occupancy of transcriptionally upregulated mRNAs upon glucose starvation are reproducible and independent of the mRNA isolation method. Ribosomal profiling was performed on strains BY4741 and EY0690 grown in glucose-rich and glucose-starvation conditions. The fold change in ribosome occupancy versus the fold change in mRNA level 15 min after cells are transferred to medium lacking glucose is shown. Genes are represented by individual symbols on the plot. Ribosome occupancy was calculated for the coding region of each gene by dividing the total number of ribosome sequence counts in an ORF (normalized to the total number of aligned reads in RPM) by the number of mRNA sequence counts (RPM) in the same sequence. The coloured symbols in each panel show the gene classes defined from BY4741 ribosomal profiling of non-poly(A)$^+$-selected mRNA replicate 1 in **a** (identical to Fig. 1a). Red symbols denote genes that have upregulated mRNA levels (>2.5) and higher ribosome occupancy (>0.09). Blue symbols denote genes that have upregulated mRNA levels (>2.5) with lower ribosome occupancy (<−1.0). Green symbols denote genes that have decreased mRNA levels (<−1.25) during glucose limitation. While downregulated mRNAs are present at decreased levels, many of them have increased ribosome occupancy, and this subset of mRNAs is enriched for genes involved in ribosome biogenesis (26 of 84; false discovery rate (FDR)-adjusted $P = 9.9 \times 10^{-4}$) by gene ontology analysis. Similarly, it has previously been observed that ribosome biogenesis mRNAs are present at decreased levels and have increased polysome association during early glucose starvation[3]. Black symbols represent all other genes in the genome for which measurements were obtained. The upregulated, higher ribosome occupancy genes (*HSP30*, *HSP26*, *HSP12* and *HSP104*) and the upregulated, lower ribosome occupancy genes (*GLC3*, *GSY1*, *GPH1* and *HXK1*) are labelled in each panel. **a**, BY4741 non-poly(A)$^+$-selected RNA, ribosome profiling replicate 1 (same as Fig. 1a). **b**, EY0690 non-poly(A)$^+$-selected RNA, ribosome profiling replicate 1. **c**, BY4741 poly(A)$^+$-selected RNA, ribosomal profiling replicate 1. **d**, EY0690 poly(A)$^+$-selected RNA, ribosome profiling replicate 1. **e**, BY4741 poly(A)$^+$-selected RNA, ribosomal profiling replicate 2. **f**, EY0690 poly(A)$^+$-selected RNA, ribosomal profiling replicate 2.

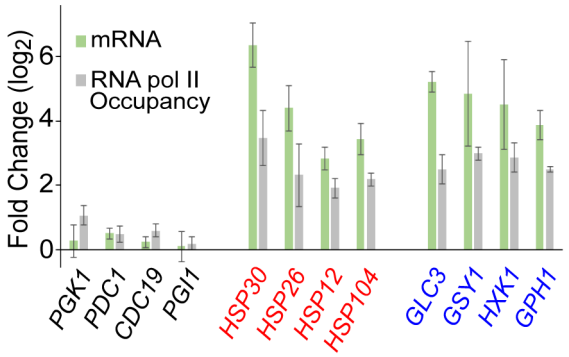

Extended Data Figure 3 | The genes corresponding to upregulated mRNAs have increased RNA polymerase II occupancy upon glucose starvation. The mRNA levels of the indicated genes were measured by RNA sequencing (RNA-seq) after 15 min of glucose starvation, and these levels were divided by the levels obtained during growth in glucose-rich medium to obtain the fold-change values. The measurements were made on independent biological samples (with strains BY4741 and EY0690), and the values are presented as the mean ± s.e.m. The RNA polymerase II occupancy was measured after 15 min of glucose starvation, and then this occupancy was divided by the occupancy in glucose-rich medium to obtain the fold-change values. RNA polymerase II occupancy was calculated from three independent biological replicates of BY4741, and the values are presented as the mean ± s.e.m.

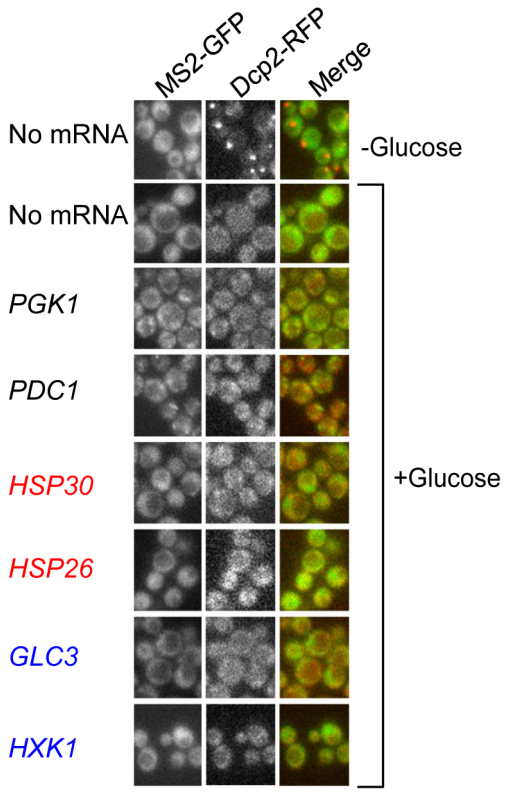

Extended Data Figure 4 | Formation of mRNA foci is dependent on MS2-binding sites and does not occur in cells growing exponentially in medium containing glucose. In the absence of mRNA containing MS2-binding sites, MS2–GFP remained diffusely localized during glucose starvation (first two rows, first column). When glucose was present in the medium, MS2 mRNA and the P body marker Dcp2–RFP were diffusely localized during the logarithmic phase of growth.

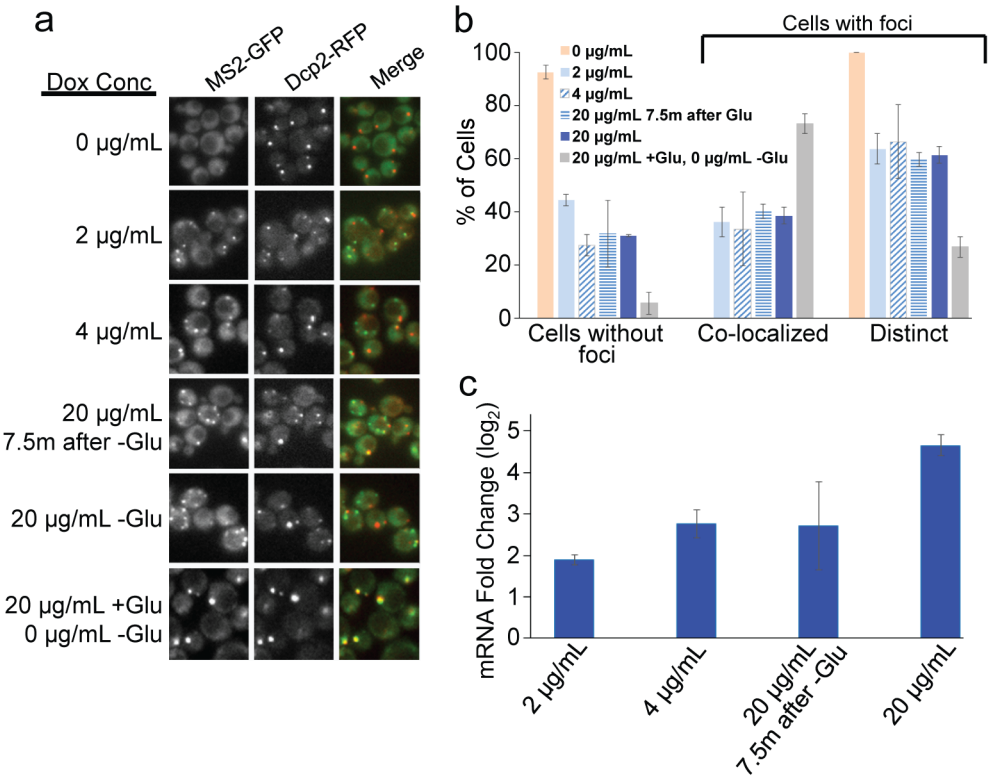

Extended Data Figure 5 | Timing of *lacZ-MS2* induction relative to glucose starvation affects mRNA localization, whereas timing or level of induction during glucose starvation has no effect. The expression of *lacZ-MS2* was either uninduced (0 µg ml^{-1}), induced to different extents with varying concentrations of doxycycline during glucose starvation (2, 4 or 20 µg ml^{-1}), induced at different times during glucose starvation (7.5 min of glucose starvation with no doxycycline, then 20 µg ml^{-1} doxycycline for the final 7.5 min of glucose starvation) or induced before glucose starvation (20 µg ml^{-1} doxycycline during logarithmic phase and none during glucose starvation) in the EY2897 strain. **a**, Localization of the mRNA was visualized using MS2–GFP after 15 min of glucose starvation for all strains. Dcp2–RFP was used to visualize P body localization. *lacZ-MS2* expression before glucose starvation caused high co-localization with P bodies, while mRNA induction during glucose starvation caused the formation of mRNA foci that both co-localized with P bodies and were distinct from P bodies. **b**, Quantification of the localization data shown in **a**. The values are presented as the mean ± s.e.m. and were calculated as follows: in quadruplicate (two biological replicates with two technical replicates per sample) for 0, 2, 20 µg ml^{-1} doxycycline in the absence of glucose and 20 µg ml^{-1} doxycycline in the presence of glucose; and in triplicate on technical replicates for 4 and 20 µg ml^{-1} doxycycline 7.5 min after the removal of glucose. **c**, Quantification of *lacZ-MS2* mRNA levels 15 min after glucose starvation. The fold change was calculated compared with the uninduced sample (0 µg ml^{-1} doxycycline) and normalized to *ACT1* abundance, as calculated from three independent biological replicates.

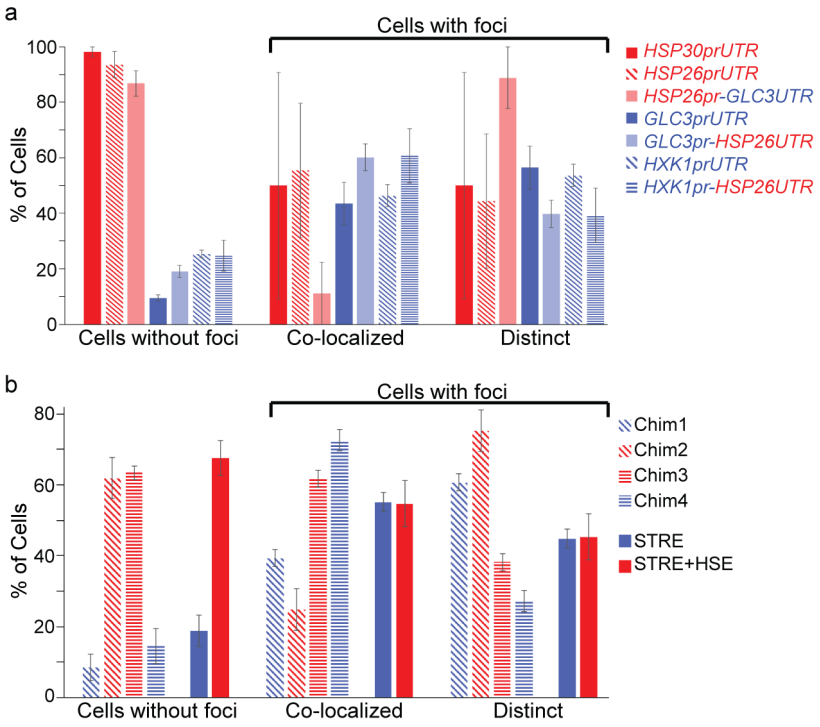

Extended Data Figure 6 | Promoter sequences determine mRNA localization upon glucose starvation. **a**, The promoter and 5′ UTR of the indicated genes were fused upstream of *CFP–MS2* in the plasmid pRS305 and integrated into EY0690. The mRNA localization was measured after 15 min of glucose starvation. The values are presented as the mean ± s.e.m. from Fig. 3c as calculated on a minimum of 30 cells in quadruplicate (two biological replicates with two technical replicates per sample). **b**, Localization of *CFP–MS2* mRNAs driven by chimaeric *HSP26* and *GLC3* promoters or synthetic (STRE or STRE+HSE) promoters upon glucose starvation. The values are presented as the mean ± s.e.m. from Fig. 4b as calculated on a minimum of 25 cells in quadruplicate (two biological replicates with two technical replicates per sample).

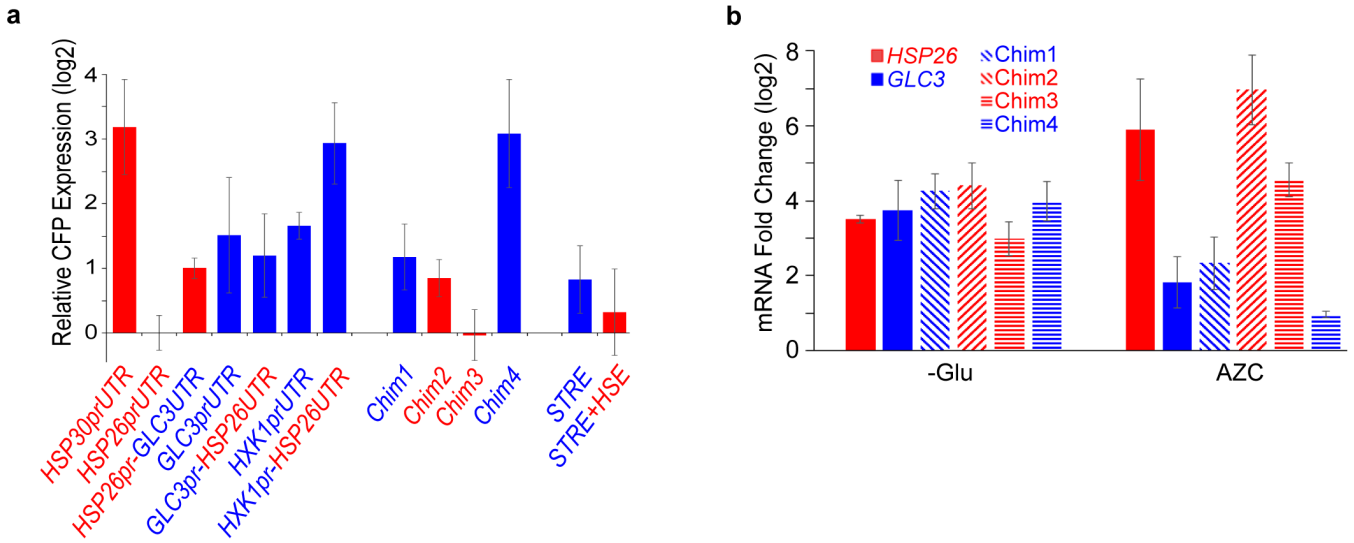

Extended Data Figure 7 | mRNA levels of *CFP–MS2* under different conditions controlled by various promoter–UTR combinations. **a**, The relative levels of *CFP–MS2* mRNA, under the control of the indicated promoter and UTR regions 15 min after glucose starvation, as measured by qPCR. The values are normalized to *ACT1* abundance and are presented as the mean ± s.e.m. relative to the *HSP26prUTR-CFP* levels and calculated from three independent biological replicates. **b**, Fold change in *CFP–MS2* mRNA abundance after 15 min of glucose starvation (−Glu) or after treatment with 10 mM AZC for 2 h (+AZC), relative to levels during logarithmic-phase growth in glucose-rich medium. *CFP–MS2* mRNA was measured by qPCR and normalized to *ACT1* levels. The values are presented as the mean ± s.e.m. as calculated from three independent biological replicates.

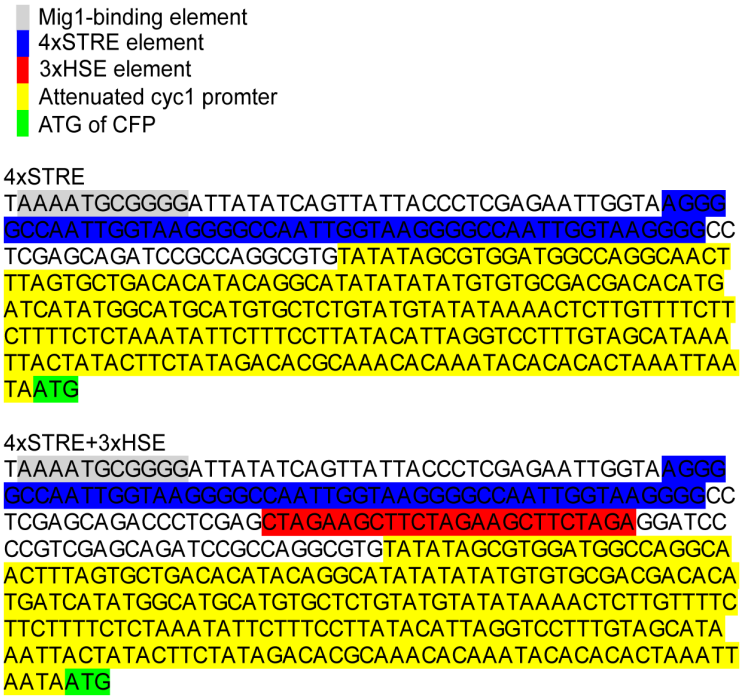

Extended Data Figure 8 | Synthetic STRE±HSE promoter sequences. The STRE±HSE elements were placed upstream of an attenuated *CYC1* promoter[17] driving the expression of *CFP–MS2*. A Mig1-binding element was included upstream of the promoter elements to reduce expression pre-starvation. The Mig1-binding element is shown in grey; the 4× STRE is labelled in blue; the 3× HSE is labelled in red; and the *CYC1* promoter is labelled in yellow.

Extended Data Table 1 | Gene ontology analysis of the classes of genes that are differentially regulated in glucose starvation

BY4741			EY0690		
Upregulated Higher-Ribo n=26	**Genes**	**p-value**	**Upregulated Higher-Ribo n=36**	**Genes**	**p-value**
Response to temperature stimulus	14	1.3E-9	**Response to abiotic stimulus**	21	9.1E-12
Response to abiotic stimulus	16	2.4E-9	**Response to temperature stimulus**	18	1.7E-11
Cellular response to heat	11	1.4E-6	**Cellular response to heat**	15	9.0E-9
Vacuolar protein catabolic process	8	1.7E-3	Cellular response to stress	16	3.4E-3
Upregulated Lower-Ribo n=18			**Upregulated Lower-Ribo n=37**		
Glucose metabolic process	7	7.8E-4	**Vacuolar protein catabolic process**	10	1.4E-4
Vacuolar protein catabolic process	7	2.0E-3	Energy reserve metabolic process	7	5.9E-4
Hexose metabolic process	7	2.5E-3	Glycogen metabolic process	6	2.6E-3
			Glucose metabolic process	8	8.2E-3
Downregulated n=84			**Downregulated n=83**		
RNA modification	19	7.6E-10	**Ribosome biogenesis**	33	1.6E-13
ncRNA metabolic process	25	2.3E-5	**Ribonucleoprotein complex biogenesis**	33	8.4E-12
rRNA processing	19	9.0E-5	**rRNA processing**	24	3.9E-9
Ribonucleoprotein complex biogenesis	24	1.3E-4	maturation of SSU-rRNA	16	6.7E-9
Ribosome biogenesis	26	9.9E-4	**ncRNA metabolic process**	27	5.9E-7
RNA processing	8	1.1E-3	**RNA processing**	28	4.3E-5
Methionine biosynthetic process	8	1.1E-3	**RNA modification**	13	7.3E-4
Sulfur amino acid biosynthetic process	8	3.2E-3	maturation of 5.8S rRNA	10	2.5E-3

DAVID analysis software was used to find the Gene Ontology (GO) terms that were significantly enriched (FDR-adjusted P value $<1.0 \times 10^{-2}$) in differentially regulated groups of genes from non-poly(A)$^+$-selected RNA-seq data and ribosomal profiling replicate 1 data for each strain (mRNA upregulated, higher ribosome occupancy (red); mRNA upregulated, lower ribosome occupancy (blue); mRNA downregulated (green)). GO terms that were common to BY4741 and EY0690 are shown in bold.

Extended Data Table 2 | Transcription start sites of mRNAs produced from promoters driving differential localization and protein production

HSP26prUTR
AAAGCAAACAAACAAACTAAACAAATTAACATG
ATTAAAACAGGTATCCAAAAAAGCAAACAAACAAACTAAACAAATTAACATG
ATTAAAACAGGTATCCAAAAAAGCAAACAAACAAACTAAACAAATTAACATG
ATTAAAACAGGTATCCAAAAAAGCAAACAAACAAACTAAACAAATTAACATG
ATATCAGATCTCTATTAAAACAGGTATCCAAAAAAGCAAACAAACAAACTAAACAAATTAACATG
GLC3pr-HSP26UTR
TAAAACAGGTATCCAAAAAAGCAAACAAACAAACTAAACAAATTAACATG
ATTAAAACAGGTATCCAAAAAAGCAAACAAACAAACTAAACAAATTAACATG
ATTAAAACAGGTATCCAAAAAAGCAAACAAACAAACTAAACAAATTAACATG
GATCTCTATTAAAACAGGTATCCAAAAAAGCAAACAAACAAACTAAACAAATTAACATG
HXK1pr-HSP26UTR
ATTAAAACAGGTATCCAAAAAAGCAAACAAACAAACTAAACAAATTAACATG
ATTAAAACAGGTATCCAAAAAAGCAAACAAACAAACTAAACAAATTAACATG
ATTAAAACAGGTATCCAAAAAAGCAAACAAACAAACTAAACAAATTAACATG
TATCAGATCTCTATTAAAACAGGTATCCAAAAAAGCAAACAAACAAACTAAACAAATTAACATG
GLC3pr-GLC3UTR
AAGTATAAAGAACCGTCAAGAATAAAATG
AAGTATAAAGAACCGTCAAGAATAAAATG
AAGTATAAAGAACCGTCAAGAATAAAATG
AAACCAAGTATAAAGAACCGTCAAGAATAAAATG
AAACCAAGTATAAAGAACCGTCAAGAATAAAATG
HSP26UTR-GLC3UTR
CAAACCAAGTATAAAGAACCGTCAAGAATAAAATG
ACAAACCAAGTATAAAGAACCGTCAAGAATAAAATG
GATAAACAAACCAAGTATAAAGAACCGTCAAGAATAAAATG
ACCGATAAACAAACCAAGTATAAAGAACCGTCAAGAATAAAATG
ACCGATAAACAAACCAAGTATAAAGAACCGTCAAGAATAAAATG
STRE
ACGCAAACACAAATACACACACTAAATTAATAATG
ATAGACACGCAAACACAAATACACACACTAAATTAATAATG
ATAGACACGCAAACACAAATACACACACTAAATTAATAATG
ATACTTCTATAGACACGCAAACACAAATACACACACTAAATTAATAATG
ATACTTCTATAGACACGCAAACACAAATACACACACTAAATTAATAATG
GTAGCATAAATTACTATACTTGCATAGACACGCAAACACAAATACACACACTAAATTAATAATG
STRE+HSE
AAATTAATAATG
AAACACAAATACACACACTAAATTAATAATG
ATACTTCTATAGACACGCAAACACAAATACACACACTAAATTAATAATG
ATACTTCTATAGACACGCAAACACAAATACACACACTAAATTAATAATG
ATACTTATATAGACACGCAAACACAAATACACACACTAAATTAATAATG
ATAAATTACTATACTTCTATAGACACGCAAACACAGATACACACACTAAATTAATAATG

5′ Rapid amplification of cDNA ends (RACE) was used to determine the transcriptional start sites of the *CFP–MS2* mRNAs driven by the indicated promoter–5′ UTR combinations.